Limnol. Oceanogr., 55(2), 2010, 872–884

Control of nitrous oxide emission from *Chironomus plumosus* larvae by nitrate and temperature

Peter Stief,[a,b,*] Lubos Polerecky,[a] Morten Poulsen,[b] and Andreas Schramm[b]

[a] Max Planck Institute for Marine Microbiology, Microsensor Group, Bremen, Germany
[b] Department of Biological Sciences, Microbiology, Aarhus University, Aarhus, Denmark

Abstract

Aquatic invertebrates that ingest large numbers of bacteria produce substantial amounts of the greenhouse gas N_2O because of incomplete denitrification in their anoxic gut. We investigated the influence of two key environmental factors, temperature and NO_3^- availability, on N_2O emission from larvae of *Chironomus plumosus* in field and laboratory experiments. Larvae collected from lake sediments emitted between 2 and 73 pmol N_2O ind.$^{-1}$ h^{-1} during the warm season, but took up maximally −27 pmol N_2O ind.$^{-1}$ h^{-1} during winter. Larvae kept in laboratory microcosms emitted between 14 and 122 pmol N_2O ind.$^{-1}$ h^{-1}, and N_2O uptake was never observed. For both types of larvae, the rate of N_2O emission was stimulated by temperature (when the NO_3^- concentration in the water column was higher than 25–50 μmol L^{-1}) and by NO_3^- (when the temperature was higher than 4–10°C). Modeling based on experimentally determined ventilation parameters and sedimentary O_2 and NO_3^- turnover rates predicted that NO_3^- concentrations inside the burrow and in the sediment surrounding the burrow fluctuated and were on average lower than those in the water column. In contrast, NO_3^- concentrations measured in the gut and hemolymph of the microcosm-incubated larvae were at least as high as in the water column. This suggests that N_2O emission from *C. plumosus* larvae is controlled by NO_3^- availability in the water column, but is decoupled, by a hitherto unknown mechanism, from NO_3^- present in the immediate surroundings of the larva.

Nitrous oxide emission from freshwater sediment is enhanced in the presence of benthic invertebrates (Svensson 1998). Recently, it has been discovered that a considerable fraction of this enhancement is due to N_2O production directly associated with the animals (Stief et al. 2009). Filter- and deposit-feeding aquatic invertebrates (FD feeders) in particular emit substantial amounts of this potent greenhouse gas. All of the FD-feeding species that have so far been proven to emit N_2O often occur at abundances of several thousand to tens of thousands of individuals per square meter (Wright et al. 1981; Svensson and Leonardson 1996; Ricciardi et al. 1997). Hence, these animals have the potential to significantly enhance the rate of N_2O emission from aquatic ecosystems. N_2O is produced in the gut of FD feeders because of incomplete denitrification by bacteria that have been ingested together with food particles (Stief et al. 2009). Animal guts in which denitrification and concomitant production of N_2O occur are characterized by anoxia and the availability of NO_3^- and dissolved organic substrates (Horn et al. 2003; Stief and Eller 2006). Thus, many of the ingested soil and sediment bacteria experience a shift from oxic conditions in their natural environment to anoxic conditions in the animal gut, which induces denitrification and N_2O production (Horn et al. 2003; Stief et al. 2009).

Although the link between the N_2O emission and the feeding traits of the animals involved has been established, the question remains as to what extent environmental factors control the rate of N_2O emission from aquatic invertebrates. In this context, the influence of the environmental factors must be considered at two scales: macroscopic, corresponding to the animal's habitat at large, and microscopic, representing the immediate surroundings of the animal and even body compartments of the animal itself. The availability of NO_3^- in the animal's macroenvironment is largely determined by the type of ecosystem in which it lives, the degree of pollution with NO_3^-, and the season (Wall et al. 2005; Pina-Ochoa and Alvarez-Cobelas 2006; Dahnke et al. 2008). On the other hand, the microenvironmental conditions with respect to NO_3^- availability can, within certain limits, also be influenced or controlled by the animal itself. For example, the periodic ventilation of the burrow for the purpose of respiration and filter feeding flushes the burrow with NO_3^- from the water column (Kristensen et al. 1991; Stief and De Beer 2006). This NO_3^- diffuses into the sediment surrounding the burrow, where it is consumed by denitrifying bacteria, resulting in a potentially significant sink for NO_3^- in the burrow (Nielsen et al. 2004). However, it is unclear whether the bacteria in the animal gut must compete against this sink, or whether the ventilation of the burrow by the animal is efficient enough to maintain sufficiently high NO_3^- concentrations in the burrow and the observed rate of N_2O emission from the animals.

Temperature is another key environmental factor that probably influences the rate of N_2O emission from aquatic invertebrates. The most obvious is the direct control of the metabolic rate of denitrifying bacteria in the animal gut. Additionally, the seasonal change in temperature affects the rate of NO_3^- consumption by denitrifying bacteria in the sediment and, together with light, also that of pelagic and benthic primary producers (Jørgensen and Sørensen 1985; Pina-Ochoa and Alvarez-Cobelas 2006). The seasonal and diel change in temperature also affects the rates of

* Corresponding author: pstief@mpi-bremen.de

respiration, feeding, and burrow ventilation of sediment-dwelling invertebrates (Leuchs 1986; Hymel and Plante 2000; Wang et al. 2001). Hence, temperature is expected to exert also an indirect control on the rate of N_2O emission from aquatic invertebrates, namely via control of NO_3^- availability in the water column, inside the burrow, and inside the animal gut.

We investigated the effect of NO_3^- availability and temperature on the N_2O emission from the larvae of *Chironomus plumosus* (Insecta, Diptera), a widely distributed freshwater midge that lives in burrows reaching deep into the sediment. The larvae were either freshly collected from lake sediments or incubated in laboratory microcosms at specific NO_3^- concentrations and temperatures. Our hypothesis was that N_2O emission from *C. plumosus* larvae is controlled by temperature and NO_3^- availability in the water column. We expected that these macroenvironmental conditions determine the microenvironmental conditions for the gut bacteria of *C. plumosus* larvae that produce N_2O via incomplete denitrification. To investigate the nature of this coupling, we carried out numerical simulations of the O_2 and NO_3^- dynamics inside and around the burrow of the larva as a function of its ventilation activity.

Methods

Origin of materials—C. plumosus larvae were collected from sediments in two shallow lakes in the temperate zone. Lake Engelsholm, located in Jutland (Denmark), has a mean depth of 2.6 m and exhibits pronounced annual fluctuations of temperature (4–20°C) and NO_3^- concentrations (0–150 μmol L^{-1}). Lake Großer Binnensee, located in Schleswig-Holstein (Germany), has a mean depth of 1.9 m and also exhibits pronounced annual fluctuations of temperature (5–21°C; Deines et al. 2007) and NO_3^- concentrations (0–130 μmol L^{-1}; Sommer 1989). In Lake Engelsholm, fourth-instar larvae were sieved from sediment collected with an Ekman grab and then used immediately for N_2O measurements under in situ conditions. In Lake Großer Binnensee, fourth-instar larvae were collected on several occasions and kept at 15°C and in the dark until used in laboratory experiments within 2 weeks. Also, the sediment for these laboratory experiments was collected in Großer Binnensee and stored at 4°C in the dark until used within 2 months. Water samples for $NO_3^- + NO_2^-$ analysis were taken in Lake Engelsholm and analyzed by the Environmental Center Ribe (Denmark). For this purpose, water samples taken at 1× and 2× Secchi depths were combined. During the time of this study, the Secchi depth varied between 1.05 and 3 m.

Field investigation—C. plumosus larvae and lake water from Lake Engelsholm were sampled monthly from October 2006 to October 2007. Directly on the shore, 10 larvae were gently washed in sterile-filtered lake water (0.20 μm, Sartorius) and individually placed in 3-mL blood collection vials (Terumo). The vials were completely filled with sterile-filtered lake water, sealed gas-tight with a butyl stopper, and incubated at in situ temperature. Subsamples of 1 mL were transferred in 1.5-h time intervals from each vial to a new, N_2-flushed vial in which the biological activity was inhibited by 50 μL of a saturated $ZnCl_2$ solution. After each sampling, the vials were immediately pressure-equalized by inserting a hypodermic needle through the stopper for < 3 s. In the laboratory, the N_2O concentration in the vials containing the 1-mL subsamples was measured by injecting 0.3 mL of headspace into a gas chromatograph with a ^{63}Ni electron capture detector (Shimadzu GC-8A). Calibration standards of 0–25 ppm N_2O in N_2 were prepared by adding known amounts of N_2O to N_2-flushed septum vials of known volume. The detection limit of the gas chromatograph was 0.3 ppm N_2O and the analytical precision of the measurements was 0.1 ppm. The linear increase of N_2O concentration during the 3-h incubations was used to calculate the rate of N_2O emission per specimen. The rate obtained by this approach corresponds to a potential rate, because the larvae were incubated in lake water and thereby may have been exposed to higher NO_3^- concentrations than in their burrows. For each sampling date, the temperature and the concentrations of NO_3^- and N_2O in the lake water were also measured.

Laboratory experiments—Twelve 600-mL glass beakers were filled with 500 mL lake sediment, 100 mL tap water, and 10–15 *C. plumosus* larvae. Within 2 d, the larvae established steady, 10-cm-deep burrows in the sediment. The beakers were submersed in 12-liter aquaria filled with 10 liters aerated tap water. Tap water was used because of its low NO_3^- concentration (10 μmol L^{-1}), which made it suitable for NO_3^- addition experiments. Four aquaria each were incubated at 4°C, 15°C, and 21°C. For each temperature, the NO_3^- concentration of the tap water was adjusted to 10, 50, 250, and 500 μmol L^{-1} using a 1 mol L^{-1} $NaNO_3$ stock solution. This set of treatments covered a wide range of environmental conditions that *C. plumosus* larvae typically encounter in both their lake and stream habitats. In this experimental setup, *C. plumosus* larvae were studied with respect to N_2O emission, NO_3^- concentration in hemolymph and gut, and ventilation parameters. Additionally, the setup served to study lake sediment with respect to O_2 and NO_3^- turnover rates.

N_2O emission rates of individual larvae were measured in 3-mL gas-tight vials that contained the larva, 100 μL of sterile-filtered water from the respective aquarium to keep the vial moist, and air as headspace (Stief et al. 2009). The larvae were moving around in the incubation vial without being directly exposed to the NO_3^- in the minute volume of aquarium water. The sealed vials were incubated at the respective temperatures, and 3 or 4 headspace samples (0.8 mL) were withdrawn with a gas-tight syringe at time intervals of 1 h for N_2O analysis by gas chromatography. Each headspace sample withdrawn was immediately replaced with air, which represented a dilution of the headspace that was corrected for. The linear increase of N_2O concentration during the incubation was used to calculate the rate of N_2O emission per specimen. The rate obtained by this approach corresponds to an actual rate, because the production of N_2O in the animal gut was fueled

exclusively by NO_3^- that the animals had taken up while still being in their burrows.

NO_3^- concentrations in the hemolymph and the gut contents were determined in freshly killed *C. plumosus*. Larvae were decapitated with a scalpel and the gut quickly pulled out with forceps. The gut contents enclosed by the peritrophic membrane were pulled out of the gut epithelium and collected in 100 μL deionized water in a centrifuge tube placed on ice. The tubes were vigorously shaken to disperse the gut contents and centrifuged at 12,100 $\times$ *g* and 4°C, and the supernatant was collected in a fresh tube that was stored at −20°C. In the meantime, 5 μL of hemolymph leaking out of the decapitated larva was collected in 50 μL deionized water in a centrifuge tube and stored at −20°C. NO_3^- concentrations were measured with the VCl_3 reduction method (Braman and Hendrix 1989) combined with NO analysis on a chemiluminescence detector (CLD 86, EcoPhysics). Five microliters of sample was injected into the reaction chamber operated at 85°C for conversion of NO_3^- and NO_2^- to NO. NO_2^- concentrations were always lower than 1 μmol L^{-1}, as measured with the reaction chamber operated at 21°C. For the calculation of in vivo concentrations of NO_3^-, the dilution with deionized water as well as the water contents of the filled gut (85%) was considered.

Ventilation activity of the *C. plumosus* larvae in sediment cores was determined by the O_2 imaging method described previously (Polerecky et al. 2006). A square core ($\sim$ 15 $\times$ 15 $\times$ 25 cm) containing a transparent polycarbonate window equipped with a planar O_2 optode ($\sim$ 7 $\times$ 15 cm, 20 μm thick) was filled with lake sediment and tap water, which was continuously flushed with air. A thin plastic barrier was inserted $\sim$ 2 cm from the optode, and the core was incubated for several days at 15°C to equilibrate. Afterwards, 10–15 *C. plumosus* larvae were placed in the volume confined by the barrier and the window. Within 2–3 d, larvae created steady burrows, few of which were close to the planar optode. O_2 images in the sediment around these burrows were recorded in 15-s intervals while the cores were progressively incubated for 2 d at experimental temperatures 15°C, 4°C, 15°C, 21°C, 4°C, and 21°C. Durations of the pumping events (t_{PE}) and resting periods (t_{RP}), defined as the time intervals during which the measured O_2 around the burrow increased and decreased, respectively (Polerecky et al. 2006), were first averaged for each individual burrow and then averaged over all observed burrows at each experimental temperature. The values of t_{PE} and t_{RP} determined during the transition periods (3–5 h) from one temperature to the next were disregarded.

Velocity of the water flow inside the burrow during the pumping events (PEs) was determined by a fluorescence imaging method. Sediments with *C. plumosus* larvae were incubated for at least 5 d in glass beakers at experimental temperatures 4°C, 15°C, and 21°C. After an equilibrium was established, a fluorescent dye (10 mg L^{-1} fluorescein) was gently injected above the burrow neighboring the glass wall and the fluorescence intensity was imaged in 1-s intervals using pulsed ($\sim$ 40 ms) illumination with a blue light-emitting diode (λ_{max} = 455 nm, Lumileds). Velocity of the water flow was calculated from the spatial progression of the dye front along the burrow in time, as determined by processing of 5–10 images recorded subsequently during the PE. The dye was injected above the burrow for each replicate measurement. The average velocities for each experimental temperature were calculated from the mean values determined for each individual burrow.

O_2 and NO_3^- consumption rates in the sediment were obtained by microsensor profiling and modeling (*see* below). Microsensors for O_2 and NO_3^- (Revsbech 1989; Sweerts and De Beer 1989) were simultaneously used in a measuring setup as described previously (Stief and De Beer 2002). At least three vertical steady-state concentration profiles per sediment beaker were recorded from 2 mm above to 10 mm below the sediment surface.

Numerical simulations—A diffusion–reaction model was developed and implemented in Matlab (version 7, MathWorks) to simulate the coupled O_2 and NO_3^- dynamics inside and around a cylindrical burrow induced by ventilation activity of the larva. The aim was to estimate the effects of a given sequence of pumping and resting intervals and of the sedimentary uptake of O_2 and NO_3^- on the magnitude of O_2 and NO_3^- fluctuations inside the burrow lumen.

Modeling was done in a cylindrical system of coordinates (axial dimension [*z*], radial distance [*r*], axial angle [φ]), employing a regular grid in the *r* and *z* directions (grid step δr and δz) and a uniform time step (δt). The burrow was approximated by a cylinder of radius r_0, starting at position $z = 0$, which corresponded to the sediment surface, and extending in the positive *z* direction, i.e., into the sediment, towards infinity. Because of the assumed cylindrical symmetry, concentrations of O_2 and NO_3^-, denoted as *c* and *e*, respectively, were considered only functions of *z*, *r*, and time (*t*), i.e., were independent of φ.

During the resting period (RP), we assumed that the water inside the burrow lumen was stagnant and thus the solute transport in and around the burrow was governed by diffusion. Consequently, the dynamics of *c* and *e* followed the diffusion–reaction equations

$$\frac{\partial c}{\partial t} = D_c \Delta c - R_c(c) \tag{1a}$$

$$\frac{\partial e}{\partial t} = D_e \Delta e - R_e(e, c) \tag{1b}$$

Here, the Laplacian operator expressed in cylindrical coordinates takes the form $\Delta = (1/r)\partial/\partial r + \partial^2/\partial r^2 + \partial^2/\partial z^2$ (the derivative with respect to φ was zero because of axial symmetry). The diffusion coefficients of O_2 (D_c) and NO_3^- (D_e) were assumed to be constant throughout the calculation domain, which was reasonable because of the very high water content of the sediment (85%). The values of R_c and R_e inside the burrow ($r \le r_0$, for all positive *z*) and in the overlying water were set to zero. In the sediment surrounding the burrow, the volume-specific O_2 (OCR) and NO_3^- (NCR) consumption rates were assumed to follow the Michaelis-Menten law with respect to the corresponding substrates, with NCR being additionally

inhibited by O_2 in a reversible and noncompetitive manner (Bergethon 1998). Thus, OCR and NCR were expressed as (Soetaert et al. 1996; Brand et al. 2009)

$$R_c(c) = OCR_{\max} \frac{c}{c + K_m^{O_2}} \tag{2a}$$

$$R_e(e, c) = NCR_{\max} \frac{e}{e + K_m^{NO_3^-}} \left(1 - \frac{c}{c + K_i^{O_2}}\right) \tag{2b}$$

where K_m and K_i denote the affinity constants towards the substrate and the inhibitor, respectively. The maximum rates as well as the affinity constants used in these expressions were estimated by fitting the steady-state microsensor profiles measured at the sediment surface with this model (results summarized in Table 1).

During the pumping interval, c and e in the sediment surrounding the burrow ($r > r_0$) were assumed to follow the same diffusion–reaction model (Eqs. 1, 2). Pumping of water was realized by moving the water volume inside the burrow downward by a z step of $z_s = v\delta t$, where δt was the time step of the numerical calculation and v was the flow velocity. Technically, this was done by setting the concentration profiles at time $t + \delta t$ and at positions $z + z_s$ to those at time (t) and at positions (z), i.e., $c(r, z + z_s, t + \delta t) = c(r, z, t)$ and $e(r, z + z_s, t + \delta t) = e(r, z, t)$, for all $r \leq r_0$ before numerically applying the time step governed by Eqs. 1, 2.

With respect to boundary conditions, the concentrations at the sediment–water interface, i.e., at $z = 0$ and for all r, were fixed to the corresponding values in the overlying water (c_w and e_w; Table 1) during both pumping and resting intervals. A zero-flux boundary condition was applied at the boundaries of the radial coordinate, i.e., at $r = r_{\max}$. Furthermore, $r_{\max}$ was set sufficiently large to ensure that c and e remained zero at all times and at all depths greater than the O_2 and NO_3^- penetration depths calculated close to the sediment–water interface. The flux at the bottom of the calculation domain, i.e., at $z = z_{\max}$, was set equal to that at $z_{\max} - \Delta z$. Because $\Delta z \ll z_{\max}$, this approximation had no effect on the calculated dynamics.

Two additional assumptions were considered in the model. First, the larval respiration as well as possible direct effects of the larva on NO_3^- turnover inside the burrow were neglected, because the model aimed at estimating the influence of the surrounding sediment on O_2 and NO_3^- dynamics in the burrow lumen. Second, the diffusive boundary layer (DBL) next to the burrow wall during the pumping interval was assumed to have zero thickness. Fluxes of solutes across the sediment–water interface have been shown to decrease with an increasing DBL thickness. However, for a DBL thickness of 0.5 mm, which is a reasonable maximum in the case of a burrow with a diameter of 1.5 mm, O_2 and NO_3^- fluxes decrease, respectively, by less than $\sim$ 15% and 1–2% compared to the fluxes at zero DBL (Brand et al. 2009). Thus, the simplifying assumption of a zero DBL thickness does not affect the conclusions of this study.

Numerical simulations were performed using parameters summarized in Table 1, which were either determined

Table 1. Parameters used for modeling of burrow ventilation by *C. plumosus*.

T (°C) (Adj)	v (mm s^{-1}) (Exp)	t_{PE} (min) (Exp)	t_{RP} (min) (Exp)	$OCR_{\max}$ (μmol m^{-3} s^{-1}) (Exp)	$NCR_{\max}$ (μmol m^{-3} s^{-1}) (Exp)	D_{O_2} (10^{-9} m^2 s^{-1}) (Lit)	D_{NO_3} (10^{-9} m^2 s^{-1}) (Lit)	$O_{2,w}$ (μmol L^{-1}) (Adj)	$NO_{3,w}$ (μmol L^{-1}) (Adj)
4	2.0	15	55	24±4	14±2	1.28	1.03	409	50 or 500
15	3.7	9.2	10	29±8	17±2	1.83	1.47	314	50 or 500
21	7.8	6.7	9	60±19	35±4	2.18	1.75	278	50 or 500

T, temperature; Adj, parameter used was considered equal to that adjusted in the experiments; v, water flow velocity inside the burrow; Exp, parameter used was determined by an independent experiment; t_{PE}, duration of the pumping event; t_{RP}, duration of the resting period; OCR, volumetric O_2 consumption rate; NCR, volumetric NO_3^- consumption rate (both OCR and NCR are expressed per unit volume of sediment); D_{O_2}, diffusion coefficient of O_2; Lit, parameter used was taken from literature; D_{NO_3}, diffusion coefficient of NO_3^-; $O_{2,w}$, O_2 concentration in the water column; $NO_{3,w}$, NO_3^- concentration in the water column. Parameters $K_m^{O_2} = 1$ μmol L^{-1}, $K_m^{NO_3^-} = 10$ μmol L^{-1}, and $K_i^{O_2} = 10$ μmol L^{-1} were similar for all experimental temperatures.

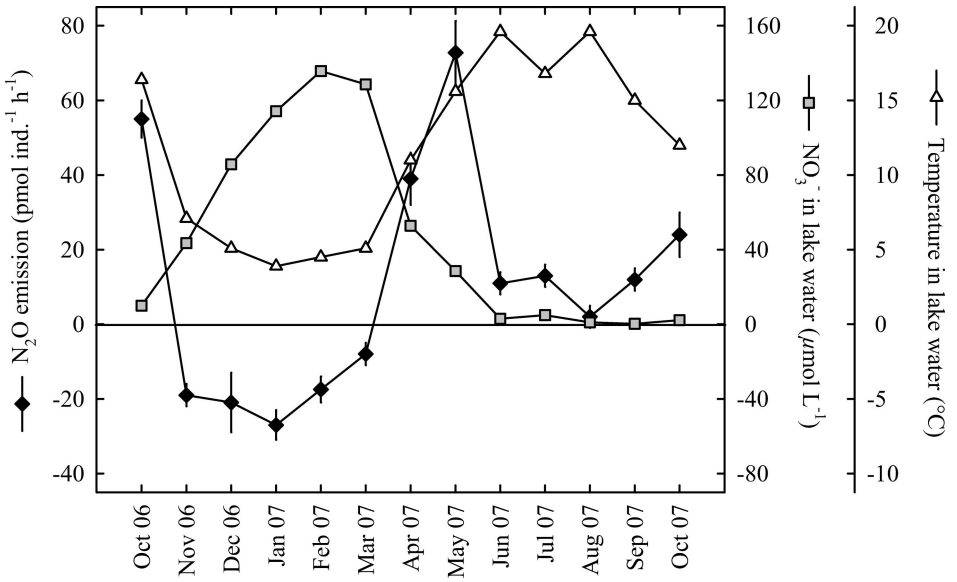

Fig. 1. Annual variation of temperature and NO_3^- concentration in Lake Engelsholm (Denmark, Jutland) and of the potential rate of N_2O emission from *C. plumosus* larvae. The potential rate of N_2O emission was determined with larvae that were freshly collected and separated from the lake sediment and incubated in lake water at in situ temperature. Means ± SE of $n = 10$ replicates are shown.

experimentally (volume-specific consumption rates, pumping and resting intervals, flow velocities, burrow radius), adjusted during experiments (NO_3^- concentrations in the water column), or taken from the literature (temperature-corrected diffusion coefficients; Broecker and Peng 1974; Li and Gregory 1974). Initially, c and e were set to zero everywhere in the sediment ($z > 0$) and equal to the overlying water concentrations at $z = 0$. Subsequently, O_2 and NO_3^- concentrations as a function of time were calculated during the succession of three PEs, each followed by an RP. The durations of the first two pumping and resting intervals were set to t_{PE} and t_{RP} (Table 1), respectively, to evaluate the dynamics under average conditions determined experimentally. To quantify the effect of a much shorter pumping and much longer resting interval, the durations of the third pumping and resting intervals were set to $t_{PE}/2$ and $2t_{RP}$, respectively. To obtain scalar quantities that reflect the temporal variations of O_2 and NO_3^- concentrations inside and around the burrow at selected depths (10 and 50 cm), the radial distributions of c and e at these depths were averaged over intervals $r \in \langle 0, r_0 \rangle$ and $r \in \langle r_0, 2r_0 \rangle$, respectively.

Results

Nitrous oxide emission from C. plumosus—Field investigation: In Lake Engelsholm, the NO_3^- concentration in the water column showed a pronounced seasonal variation, with high values during winter and low values during summer, whereas the temperature curve showed the opposite trend (Fig. 1). The potential rate of N_2O emission from *C. plumosus* larvae collected in Lake Engelsholm followed the temperature curve to some degree, but very high emission rates were observed in April and May 2007. In the warm season, the potential rate of N_2O emission ranged between 2 and 73 pmol ind.$^{-1}$ h^{-1}. In winter, however, uptake of N_2O by the larvae of up to −27 pmol ind.$^{-1}$ h^{-1} was observed. This means that the N_2O concentration of the lake water decreased during the incubation, which was not the case in control vials without larvae. Because N_2O concentrations in the lake water during these measurements ranged between 32 and 80 nmol L^{-1} (annual average 48 ± 14 nmol L^{-1}), the amount of N_2O available in the measuring vial was not limiting the larval N_2O consumption.

At NO_3^- concentrations above 25 µmol L^{-1}, the potential rate of N_2O emission was significantly positively correlated with temperature (Spearman's $R = 0.775$, $p = 0.041$), but this correlation also considered negative N_2O emission rates. At temperatures higher than 10°C, the potential rate of N_2O emission was significantly positively correlated with NO_3^- concentration (Spearman's $R = 0.593$, $p = 0.049$).

Laboratory investigation: The average rates of N_2O emission from *C. plumosus* collected from laboratory microcosms ranged from 14 to 122 pmol ind.$^{-1}$ h^{-1} and varied with both the NO_3^- concentration in the water column and the incubation temperature (Fig. 2). The emission rates increased significantly with NO_3^- concentration at 15°C and 21°C, but not at 4°C (Table 2). Furthermore, the rates increased with temperature at NO_3^- concentrations of 250 and 500 µmol L^{-1}, but not at 10 and 50 µmol L^{-1} NO_3^-.

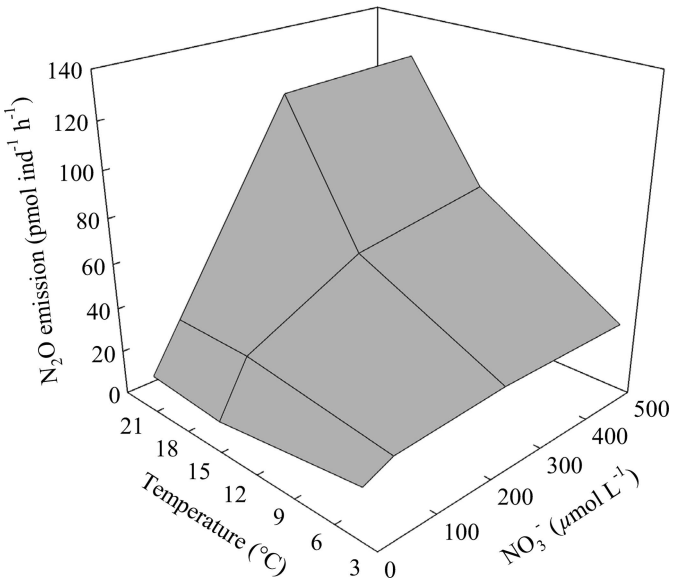

Fig. 2. Rates of N_2O emission from *C. plumosus* larvae after they were incubated for 2–4 d in laboratory microcosms at different temperatures and NO_3^- concentrations in the water column. Means of $n = 6$ replicates are shown.

Nitrate concentration in gut and hemolymph of C. plumosus—Generally, the concentration of NO_3^- in the gut and hemolymph of *C. plumosus* larvae increased with the NO_3^- concentration in the water column of the laboratory microcosms (Fig. 3). In all treatments, the average NO_3^- concentrations in the gut and hemolymph were as high as or even higher than in the water column. At 4°C and 15°C, the NO_3^- concentrations in the gut and hemolymph were in most cases not different from those in the water column (*t*-test, $T \geq -2.133$, df = 11, $p > 0.05$), whereas at 21°C, they were in most cases significantly higher than in the water column (*t*-test, $T < -2.449$, df = 11, $p < 0.05$), which must be caused by NO_3^- production or accumulation in the larvae (*see* Discussion).

Ventilation activity of C. plumosus *and its consequences*—Because of the ventilation activity of a *C. plumosus* larva, O_2 concentrations in and around the burrow exhibited characteristic dynamics consisting of alternating periods of increase and decrease (Fig. 4). Based on these dynamics, the larval activity was divided into pumping (O_2 increase) and resting (O_2 decrease) intervals of durations t_{PE} and t_{RP}, respectively, as suggested by Polerecky et al. (2006). The analysis of the complete O_2 time series, which lasted 4 d at each experimental temperature, revealed that t_{PE} and t_{RP} varied considerably within the time series for each observed burrow as well as among the different burrows observed at each temperature (*see* symbols with their corresponding

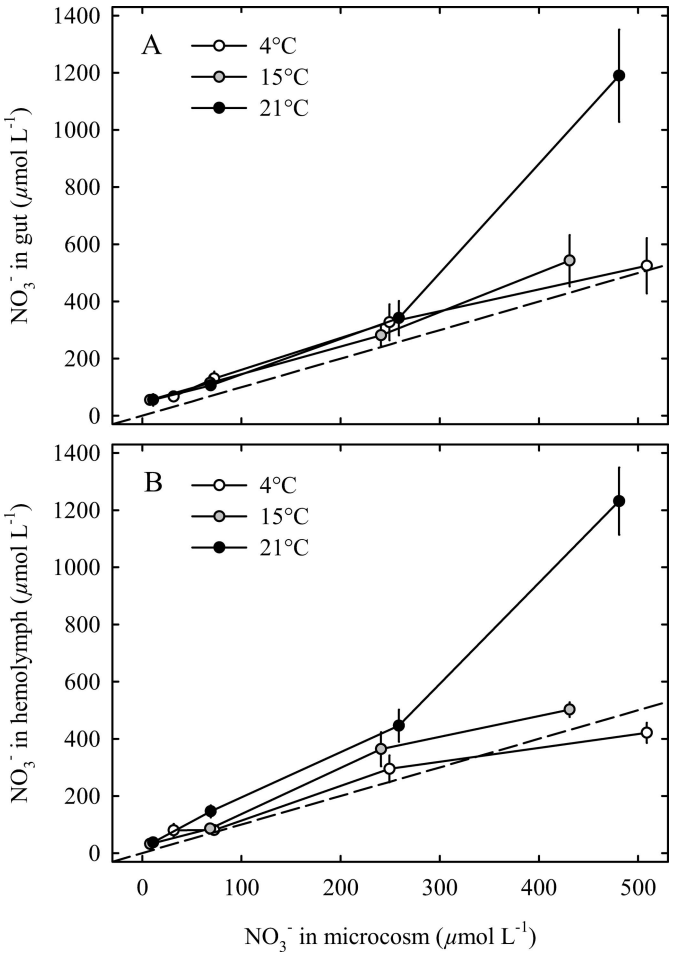

Fig. 3. NO_3^- concentration in (A) the gut and (B) the hemolymph of *C. plumosus* larvae incubated in laboratory microcosms at different temperatures and NO_3^- concentrations in the water column. The dotted line indicates identical concentrations in the water column and in the gut and hemolymph. Means ± SE of $n = 12$ replicates are shown.

Table 2. Correlations between larval N_2O emission rate and NO_3^- concentration in the water column (left columns) and between larval N_2O emission rate and temperature (right columns).

	N_2O emission rate vs. NO_3^- concentration			N_2O emission rate vs. temperature	
Temperature	*R*	*p*	NO_3^- concentration	*R*	*p*
4°C	−0.057	0.815	10 µmol L^{-1}	−0.401	0.196
15°C	0.612	0.010	50 µmol L^{-1}	−0.055	0.858
21°C	0.542	0.014	250 µmol L^{-1}	0.686	0.003
			500 µmol L^{-1}	0.860	<0.001

N_2O emission rate vs. NO_3^- concentration: Pearson's correlation coefficient *R* and the level of probability *p* are given; $n = 17$–24. N_2O emission rate vs. temperature: Spearman's correlation coefficient *R* and the level of probability *p* are given; $n = 12$–20.

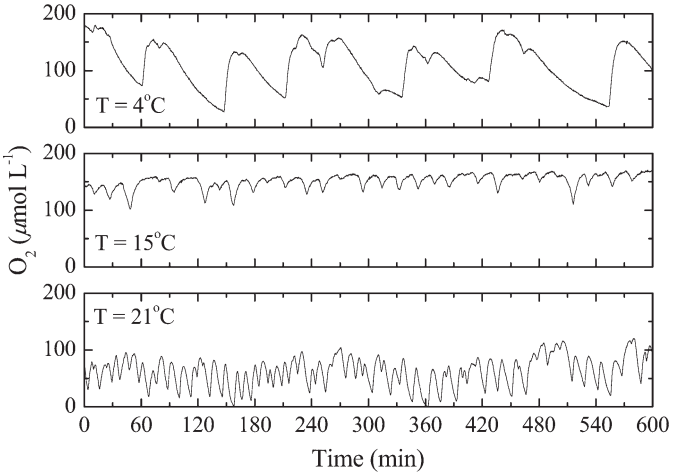

Fig. 4. Time series of the O_2 concentration close to the burrow of a *C. plumosus* larva, as determined with the oxygen imaging method at three experimental temperatures. Typical examples of concentrations measured at depths 2–3 cm below the sediment surface are shown. Note that the absolute values of the measured O_2 concentrations depend on the distance between the burrow and the planar optode, and thus do not reflect directly the O_2 concentrations inside the burrow. Thus, data like these were used only to quantify temporal aspects of the burrow ventilation.

error bars in Fig. 5A,B). When considering different burrows separately, variability of t_{PE} was similar for all temperatures (between 2 and 9 min), whereas variability of t_{RP} enormously increased to 20–55 min at 4°C compared to that at 15°C and 21°C (2–9 min). When averaged over all observed burrows, t_{PE} decreased with temperature (Fig. 5A), whereas t_{RP} enormously increased at 4°C compared to t_{RP} at 15°C and 21°C (Fig. 5B). The fluorescent dye imaging experiment revealed a similarly high degree of variability of the flow velocity inside a ventilated burrow when comparing individual burrows at each experimental temperature (Fig. 5C). The average velocities, however, exhibited a clear increasing trend with temperature.

Numerical simulations of O_2 and NO_3^- dynamics inside and around a ventilated burrow revealed that the average O_2 concentrations inside the burrow increased abruptly with time after the pumping started, and approached a steady-state value as the time passed (Fig. 6A–C). The delay of the abrupt increase in concentration, Δt, was related to the distance from the burrow entry, L, as $\Delta t = L/v$. The O_2 concentrations inside the burrow at the end of the average pumping interval decreased approximately linearly with L and, depending on temperature, reached 95–98% and 70–85% of the water column concentration at L = 10 and 50 cm, respectively (Fig. 7A, open symbols). After the pumping was stopped, the average O_2 concentrations inside the burrow decreased in an approximately exponential manner with time (Fig. 6A–C), reaching 50–55% (at L = 10 cm) and ~ 40% (at L = 50 cm) of the water column concentration at the end of the average RP at 15°C and 21°C (Fig. 7A, filled circles and squares, respectively). The decrease of the O_2 concentrations with L at the end of the average RP at 4°C was more pronounced, reaching ~ 10% and ~ 4% of the water column concentration at 10 and 50 cm, respectively (Fig. 7A, filled triangles). Calculated O_2 concentrations, when averaged over the sediment volume at radial distances between r_0 and $2r_0$ (r_0 is the burrow radius),

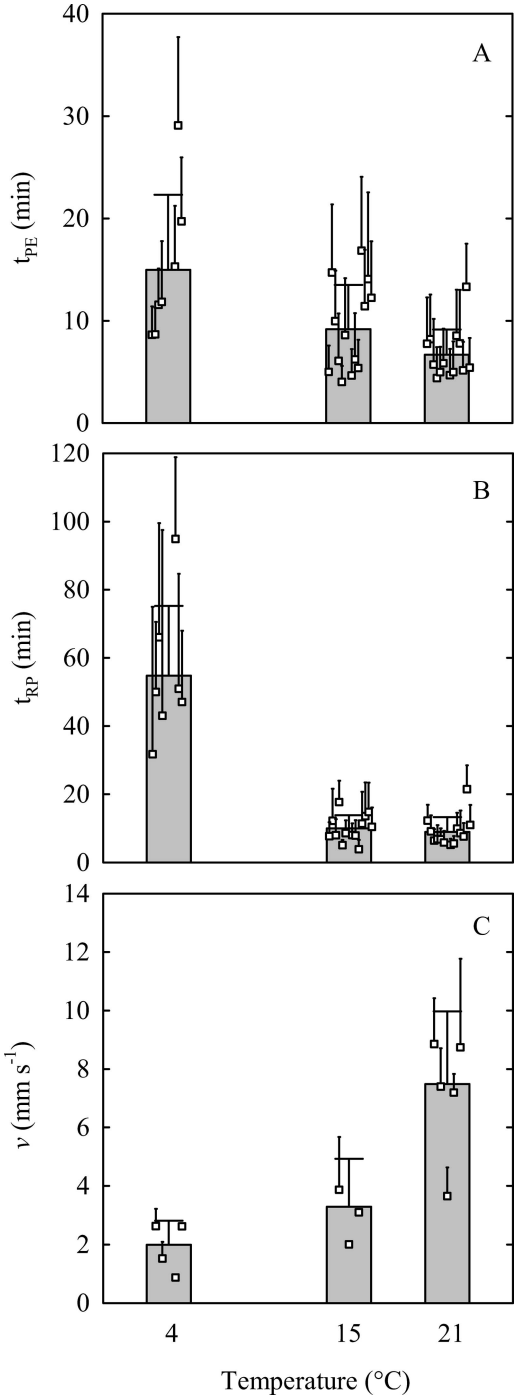

Fig. 5. Durations of (A) pumping events (t_{PE}), (B) resting periods (t_{RP}), and (C) flow velocities inside a ventilated burrow (v), as a function of temperature. Squares with error bars represent average (AV) and standard deviation (SD) calculated for individual burrows from time series lasting for several hundreds (t_{PE} and t_{RP}) and tens (v) of minutes, and columns with error bars represent total AV and SD for each experimental temperature. Note different scaling of (A) and (B).

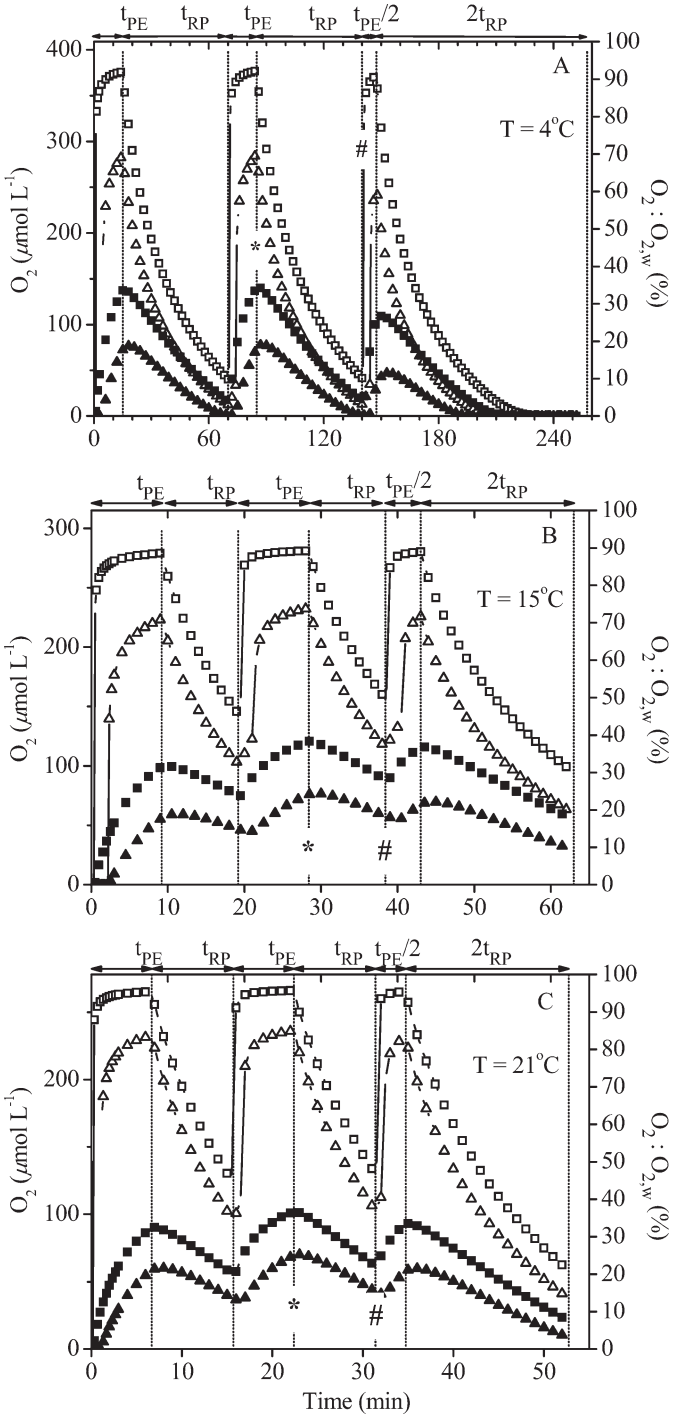

Fig. 6. (A–C) O_2 concentrations inside (averaged from 0 to r_0; open symbols) and around (averaged from r_0 to $2r_0$; filled symbols) a ventilated burrow as a function of time and temperature, modeled for 3 successive pumping and resting intervals. Squares and triangles represent the situations at distances of 10 and 50 cm from the burrow entry, respectively. Pumping and resting intervals used in the simulation are indicated by vertical dotted lines. *, end of an average pumping event; #, end of an average resting period.

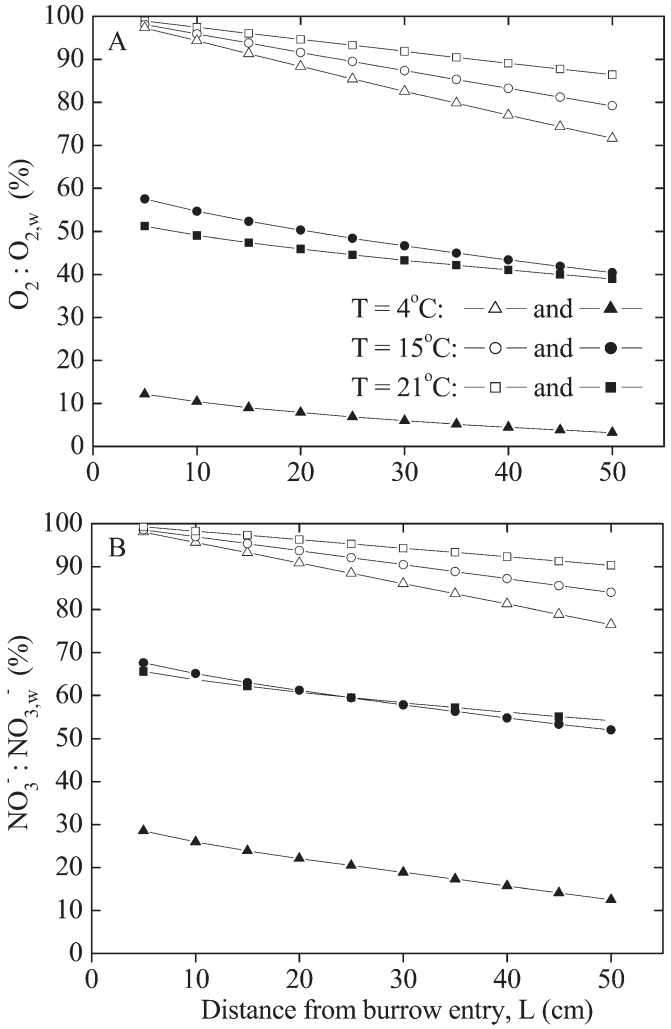

Fig. 7. (A) O_2 and (B) NO_3^- concentrations inside the burrow plotted as a function of the distance from the burrow entry at the end of an average pumping event (open symbols) and an average resting period (filled symbols). These time points are indicated in Fig. 6A–C and Fig. 8A–C by * and #, respectively. Concentrations were normalized to the concentration in the water column.

exhibited similar fluctuating patterns to those directly measured next to the burrows by the planar optode (compare Figs. 4 and 6), confirming that the approximations made and parameters applied in the modeling were realistic for the experimental settings used.

The temporal patterns seen in the simulated NO_3^- concentrations were qualitatively similar to those for O_2. Specifically, NO_3^- concentrations, at a given distance from the burrow entry, increased abruptly after the pumping started and approached a steady state with increasing time (Fig. 8A–C). At the end of the average pumping interval, NO_3^- concentrations inside the burrow decreased approximately linearly with L, and, depending on temperature, reached 95–98% and 75–90% of the water column concentration at L = 10 and 50 cm, respectively (Fig. 7B, open symbols). After the pumping was stopped, the average

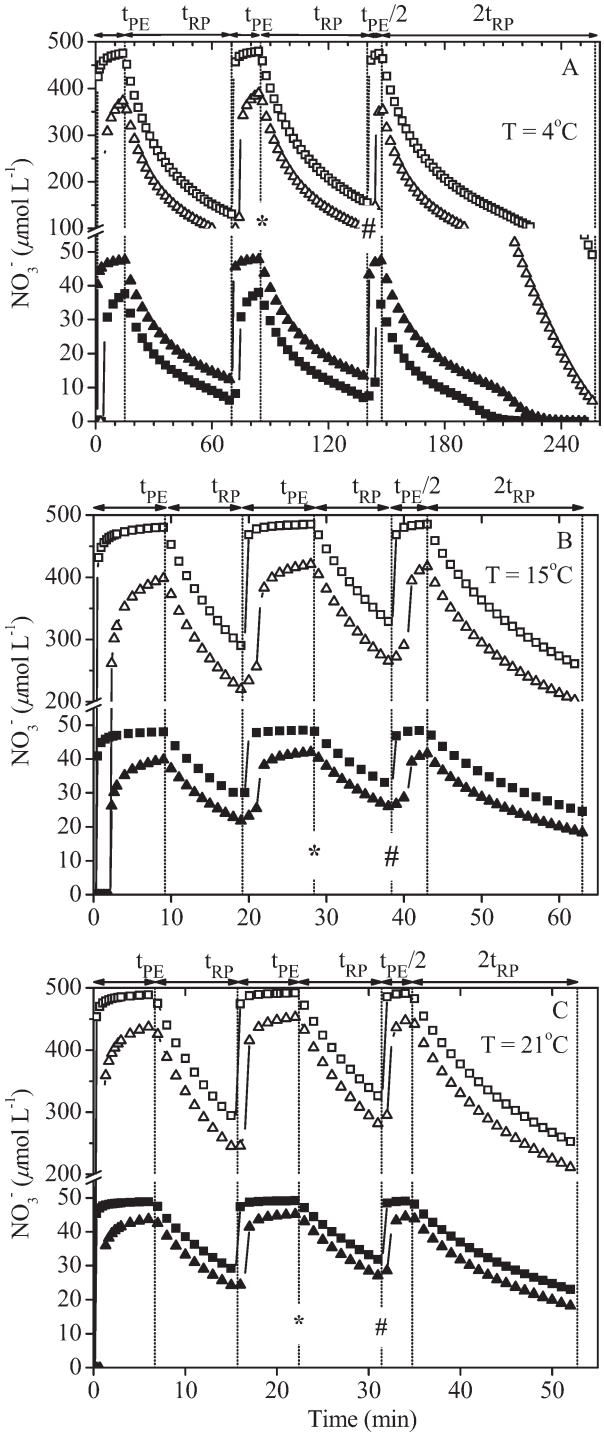

Fig. 8. (A–C) NO_3^- concentrations inside (averaged from 0 to r_0) a ventilated burrow as a function of time and temperature, modeled for 3 successive pumping and resting intervals. Squares and triangles represent the situations at distances of 10 and 50 cm from the burrow entry, respectively; open and filled symbols correspond to the overlying water NO_3^- concentrations 500 and 50 μmol L^{-1}, respectively. Pumping and resting intervals used in the simulation are indicated by vertical dotted lines. *, end of an average pumping event; #, end of an average resting period.

NO_3^- concentrations inside the burrow decreased in an approximately exponential manner with time (Fig. 8A–C), reaching ~ 65% (at L = 10 cm) and ~55% (at L = 50 cm) of the water column concentration at the end of the average RP at 15°C and 21°C (Fig. 7B, filled circles and squares, respectively). The decrease of the NO_3^- concentrations with L at the end of the average RP at 4°C was more pronounced, reaching ~ 28% and ~12% of the water column concentration at 10 cm and 50 cm, respectively (Fig. 7B, filled triangles). In general, the magnitude of the temporal variations of NO_3^- concentration inside the burrow was lower than that of the O_2 concentration. This was related to the fact that NO_3^- had to diffuse beyond the layer with high O_2 concentrations before it could be consumed at appreciable rates, leading to a delay in NO_3^- consumption relative to O_2 consumption. The simulated NO_3^- dynamics, when normalized to the NO_3^- concentrations in the water column, $NO_{3,w}$, were practically identical for $NO_{3,w}$ = 50 and 500 μmol L^{-1} (data not shown).

Discussion

N_2O emission rate vs. NO_3^- availability and temperature—The rate of N_2O emission from *C. plumosus* larvae kept in laboratory microcosms increased with the NO_3^- concentration in the water column at 15°C and 21°C, but not at 4°C. Similarly, the potential rate of N_2O emission from field-collected larvae was positively correlated with the NO_3^- concentration in the lake, but not at temperatures below 10°C. This shows that N_2O emission from the larvae is stimulated by NO_3^- availability in the macroenvironment (i.e., the water column), but only above a certain temperature threshold somewhere around 4–10°C.

The lack of stimulation of N_2O emission by NO_3^- at low temperatures cannot be explained by the lower availability of NO_3^- inside the burrow, which is predicted by numerical simulations made for laboratory-incubated larvae based on their ventilation activity, because the NO_3^- concentrations measured in the gut and hemolymph were similar to those in the water column (*see* below). Instead, the low metabolic activity of the larvae and/or the bacteria in the gut at 4°C may serve as an explanation (Bairlein 1989). At low temperature, the feeding activity of *C. plumosus* larvae is very low and the gut residence time is very long (i.e., 32 h at 5°C; Johnson et al. 1989). As a consequence, the rates of denitrification and N_2O production may become limited by dissolved organic substrates instead of NO_3^- available in the gut. Second, the gut contents of *C. plumosus* larvae might be not fully anoxic and thus not conducive to denitrification at 4°C (Stief and Eller 2006).

At 15°C and 21°C, the rate of N_2O emission increased with NO_3^- concentration and leveled off between 250 and 500 μmol L^{-1} NO_3^-, suggesting limitation of gut denitrification by dissolved organic substrates or living bacterial biomass. The larvae take up organic substrates and bacterial biomass by feeding on detritus particles trapped in a net inside the burrow (Walshe 1947), whereas NO_3^- might be taken up actively by feeding and/or passively by ion transport across the integument (Neumann et al. 2001). Because passive uptake of NO_3^- would be uncoupled from

active uptake of organic substrates and bacterial biomass, there could be a surplus of NO_3^- in the gut that cannot further increase the rate of denitrification.

The rate of N_2O emission from *C. plumosus* larvae kept in laboratory microcosms also increased with temperature, but only at NO_3^- concentrations above 50 μmol L^{-1} in the water column. Similar stimulation by temperature was observed for the field-collected larvae, but only at NO_3^- concentrations above 25 μmol L^{-1} in the water column. Clearly, gut denitrification in laboratory-incubated larvae was limited by NO_3^- availability in the gut at concentrations of 10 and 50 μmol L^{-1} NO_3^- in the water column and therefore could not be enhanced by increased temperature. Above 50 μmol L^{-1} NO_3^- in the water column, the N_2O emission rate increased exponentially with temperature, and the Q_{10} values calculated for the temperature range 4–21°C were 2.2 and 2.3 for 250 and 500 μmol L^{-1} NO_3^-, respectively. These are typical values for sedimentary denitrification (Rysgaard et al. 2004).

Taken together, NO_3^- concentration and temperature stimulated larval N_2O emission apparently only when they both exceeded certain threshold values. Such a mutual influence of NO_3^- availability and temperature is also known for sedimentary denitrification and N_2O emission (Jørgensen and Sørensen 1985; Inwood et al. 2005; Wall et al. 2005), and thus probably reflects the physiological control of denitrifying bacteria by these two variables.

Ventilation activity vs. O_2 and NO_3^- availability—C. plumosus larvae live in U-shaped burrows that may reach several decimeters deep into the sediment (Hilsenhoff 1966). The larva ventilates its burrow periodically by undulatory body movements to gain suspended food particles and O_2. Along with O_2, NO_3^- is transported into the burrow, where it is consumed by microbial processes in the surrounding sediment. To understand the coupling between the NO_3^- availability in the water column and the burrow due to the counteracting effects of burrow ventilation and denitrification activity in the burrow walls, we implemented a numerical model that takes into account the temporal aspects of larval ventilation as well as the inhibition of bacterial denitrification by O_2. This was done because NO_3^- concentrations inside the burrow could not be measured directly.

The numerical simulations suggest that the ventilation by the larva is likely triggered by a threshold O_2 concentration inside the burrow. As implied by the modeled O_2 profiles along the burrow at the end of the average resting interval (Fig. 7A), the triggering concentrations are similar at 15°C and 21°C, but are considerably lower at 4°C. This difference is mainly due to the disproportionately prolonged RPs observed at 4°C (Fig. 5B), indicating that the lower temperature significantly decreased the physiological O_2 demand of the larvae (Bairlein 1989). Simulations also show that by combining the relatively fast pumping rates and several-minute-long pumping intervals (Fig. 5), the larvae are able to effectively replenish O_2 concentrations inside the burrow to levels close to those in the overlying water (> 70%; Fig. 7A) even if burrows are up to 50 cm long.

Periodic ventilation by the larva also results in fluctuating NO_3^- concentrations inside the burrow (Fig. 8). Although the simulated range of fluctuations depended on the distance along the burrow, the concentrations were always above 50% of the water column level even for a several-decimeters-long burrow. The exception was at 4°C, where NO_3^- in deeper parts of the burrow (e.g., > 30 cm) decreased below 20% of the water column level at the end of the average RP (Fig. 7B). This implies that if the NO_3^- concentrations in the gut and hemolymph are directly coupled to the NO_3^- available in the immediate surroundings of the larva, the bacteria in the gut are not expected to be limited by NO_3^- as a consequence of denitrification activity in the sediment surrounding the burrow, except perhaps at low temperatures. This would be true regardless of whether the coupling occurs instantaneously or over time scales comparable to or larger than the typical pumping or resting intervals.

Interestingly, NO_3^- concentrations measured directly in the gut and hemolymph of *C. plumosus* larvae kept in laboratory microcosms were similar to or sometimes even higher than those in the water column, which was true for all investigated temperatures (Fig. 3). This suggests that NO_3^- in the gut and hemolymph is in fact decoupled from the NO_3^- available in the immediate surroundings of the larva, which is predicted to be fluctuating. Alternative sources of NO_3^- inside the larva or the burrow, if existing, would reconcile the predicted NO_3^- availability and the measured NO_3^- concentrations. Nitrate production in the larvae via NO dioxygenation mediated by hemoglobin (Gardner et al. 2006) could be one such possibility. This pathway converts the signaling molecule and stress hormone NO to NO_2^- and NO_3^- in vertebrate and several invertebrate species (Gardner 2005; Angelo et al. 2008), but has not yet been reported for *C. plumosus*. Alternatively, NO_3^- in the gut and hemolymph may originate from ingested and digested microorganisms that store NO_3^- intracellularly. Also, nitrification inside the burrow stimulated by larval NH_4^+ excretion could be a possible additional source of NO_3^- for the larvae. However, the probability that any of these processes would lead to equal NO_3^- concentrations in the water column and in the larva (Fig. 3) is rather low. Moreover, it is not clear whether any of these processes could quantitatively provide the internal NO_3^- surplus measured at 21°C. Thus, a conceptually different mechanism needs to be considered to explain the observed high NO_3^- concentrations in the gut and hemolymph of the larva. It can be speculated that NO_3^- is stored by the larvae during phases of high NO_3^- concentrations inside the burrow (e.g., at the end of pumping intervals). The sink constituted by the larva and its gut bacteria is not significant to deplete the internal NO_3^- during a typical RP. For example, considering a typical size of the larva (radius 1 mm, length 2 cm), the maximum observed N_2O production rate of 122 pmol $ind.^{-1}$ h^{-1} would translate to the depletion of the internal NO_3^- on the order of 4 μmol L^{-1} during a RP of 1 h, which is very little compared to the high NO_3^- concentrations measured in this study. However, NO_3^- storage by

chironomid larvae is not supported by any prior evidence and requires further investigation.

Environmental implications—The annual cycle of the potential rates determined for field-collected *C. plumosus* larvae revealed phases with positive and negative rates. Considering all field data, the net contribution of *C. plumosus* to the overall annual N_2O emission from Lake Engelsholm was estimated at 10.5 pmol ind.$^{-1}$ h^{-1}. The highest (73 pmol ind.$^{-1}$ h^{-1}) and lowest ($-$27 pmol ind.$^{-1}$ h^{-1}) rates were measured in May and January, respectively. A similar annual pattern was found for the larvae of the mayfly *Ephemera danica* that live in sandy stream sediments (P. Stief and A. Schramm unpubl.). There, the maximum rate of N_2O emission determined during spring was 2.5-fold higher than the average annual rate. Based on the average annual N_2O emission rate of field-collected *C. plumosus* larvae of 10.5 pmol ind.$^{-1}$ h^{-1} and assuming a high, but not uncommon, larval density of 5000 ind. m^{-2} in lake sediment (Fukuhara and Sakamoto 1987; Soster and McCall 1990), gut denitrification of the *C. plumosus* population will produce 0.46 mmol m^{-2} yr^{-1} of N_2O. This corresponds to 7.5–175% of N_2O emission rates reported from sediment of lakes in which *C. plumosus* might reach high densities (Mengis et al. 1997; Svensson 1998; Liikanen et al. 2003). In contrast, if the maximum N_2O emission rate determined under laboratory conditions (i.e., 122 pmol N_2O ind.$^{-1}$ h^{-1} at 21°C and 500 μmol L^{-1} NO_3^-) were used, gut denitrification by *C. plumosus* populations of the same density would annually produce 5.33 mmol m^{-2} of N_2O. It needs to be noted, however, that many lakes and reservoirs harbor densities of *C. plumosus* that are 1–2 orders of magnitude lower than used in our example (Real et al. 2000) and will therefore not exhibit a significant increase of their overall N_2O emission because of the presence of *C. plumosus* larvae.

The laboratory incubations of the *C. plumosus* larvae revealed the potential of how much the N_2O emissions from the guts of aquatic invertebrates could increase, should the environmental conditions change abruptly or gradually. For instance, heavy storms cause spates and sudden increases of NO_3^- concentrations in the water column (Rusjan et al. 2008), and may thus drastically stimulate the N_2O emission rate when NO_3^- concentrations are normally low (e.g., during warm summer and autumn months). Second, the projected increase in global temperature will increase the frequency of warm winters, potentially also leading to an increase in the N_2O emission rates due to simultaneously higher temperatures and higher wet deposition of atmospheric NO_3^- (Hole et al. 2008).

Modeling implications—By their ventilation activity, *C. plumosus* larvae supply NO_3^- from the water column to denitrifiers living in the sediment in close proximity of the burrow. Stimulation of denitrification inside chironomid burrows as well as N_2O emission from burrows by this mechanism has been shown before (Pelegri and Blackburn 1995; Svensson 1998; Stief et al. 2009). However, it has not been recognized until now that *C. plumosus* larvae are able to supply NO_3^- to the maximum depth of their burrows ($\sim$ 50 cm; Hilsenhoff 1966). In many eutrophic lakes, the densities of *C. plumosus* larvae reach several thousands of individuals per square meter (Fukuhara and Sakamoto 1987; Soster and McCall 1990). Thus, a dense and considerably deep 3-dimensional network of burrows, which are frequently flushed with NO_3^- from the water column by the ventilation activity of *C. plumosus* larvae, must exist in the sediments of these habitats. We suggest that diagenetic models, such as those developed by Meile et al. (2003) or Lewandowski and Hupfer (2005), need to incorporate these burrow networks as well as the highly dynamic input and microbial utilization of NO_3^- and other solutes to more accurately describe the biochemical exchange processes between sediments and the overlying water.

Acknowledgments

We thank Torben Wiis (Danish Ministry of the Environment, Environmental Center Ribe) for access to Lake Engelsholm and unpublished NO_3^- data. We are grateful to Gaby Eickert, Ines Schröder, and Tove Wiegers for technical assistance. The manuscript benefited from reviews by Dirk De Beer and two anonymous referees. Financial support was provided through a Marie Curie Fellowship of the European Union to P.S. (grant 515536), a Danish Research Agency Grant to A.S. (grant 2117-05-0027), European Union Project "Dynamic sensing of chemical pollution disasters and predictive modeling of their spread and ecological impact" granted to L.P. (grant 518043-1), and the Max Planck Society (Germany).

References

Angelo, M., A. Hausladen, D. J. Singel, and J. S. Stamler. 2008. Interactions of NO with hemoglobin: From microbes to man, p. 131–168. *In* R. K. Poole [ed.], Globins and other nitric oxide-reactive proteins. Pt. A. Academic.

Bairlein, F. 1989. The respiration of *Chironomus*-larvae (Diptera) from deep and shallow waters under environmental hypoxia and at different temperatures. Arch. Hydrobiol. **115:** 523–536.

Bergethon, P. R. 1998. The physical basis of biochemistry: The foundations of molecular biophysics. Springer.

Braman, R. S., and S. A. Hendrix. 1989. Nanogram nitrite and nitrate determination in environmental and biological materials by vanadium(III) reduction with chemiluminescence detection. Anal. Chem. **61:** 2715–2718.

Brand, A., C. Dinkel, and B. Wehrli. 2009. Influence of the diffusive boundary layer on solute dynamics in the sediments of a seiche-driven lake: A model study. J. Geophys. Res. **114:** G01010, doi:10.1029/2008JG000755.

Broecker, W. S., and T. H. Peng. 1974. Gas exchange between air and sea. Tellus **26:** 21–35.

Dahnke, K., E. Bahlmann, and K. Emeis. 2008. A nitrate sink in estuaries? An assessment by means of stable nitrate isotopes in the Elbe estuary. Limnol. Oceanogr. **53:** 1504–1511.

Deines, P., J. Grey, H. H. Richnow, and G. Eller. 2007. Linking larval chironomids to methane: Seasonal variation of the microbial methane cycle and chironomid d^{13}C. Aquat. Microb. Ecol. **46:** 273–282.

Fukuhara, H., and M. Sakamoto. 1987. Enhancement of inorganic nitrogen and phosphate release from lake sediment by tubificid worms and chironomid larvae. Oikos **48:** 312–320.

GARDNER, P. R. 2005. Nitric oxide dioxygenase function and mechanism of flavohemoglobin, hemoglobin, myoglobin and their associated reductases. J. Inorg. Biochem. **99:** 247–266.

———, A. M. GARDNER, W. T. BRASHEAR, T. SUZUKI, A. N. HVITVED, K. D. R. SETCHELL, AND J. S. OLSON. 2006. Hemoglobins dioxygenate nitric oxide with high fidelity. J. Inorg. Biochem. **100:** 542–550.

HILSENHOFF, W. L. 1966. The biology of *Chironomus plumosus* (Diptera: Chironomidae) in Lake Winnebago, Wisconsin. Ann. Entomol. Soc. Am. **59:** 465–473.

HOLE, L. R., H. A. DE WIT, AND W. AAS. 2008. Influence of summer and winter climate variability on nitrogen wet deposition in Norway. Hydrol. Earth Syst. Sci. **12:** 405–414.

HORN, M. A., A. SCHRAMM, AND H. L. DRAKE. 2003. The earthworm gut: An ideal habitat for ingested N_2O-producing microorganisms. Appl. Environ. Microbiol. **69:** 1662–1669.

HYMEL, S. N., AND C. J. PLANTE. 2000. Feeding and bacteriolytic responses of the deposit-feeder *Abarenicola pacifica* (Polychaeta: Arenicolidae) to changes in temperature and sediment food concentration. Mar. Biol. **136:** 1019–1027.

INWOOD, S. E., J. L. TANK, AND M. J. BERNOT. 2005. Patterns of denitrification associated with land use in 9 midwestern headwater streams. J. N. Am. Benthol. Soc. **24:** 227–245.

JOHNSON, R. K., B. BOSTRÖM, AND W. J. VAN DE BUND. 1989. Interactions between *Chironomus plumosus* L. and the microbial community in surficial sediments of a shallow eutrophic lake. Limnol. Oceanogr. **34:** 992–1003.

JØRGENSEN, B. B., AND J. SØRENSEN. 1985. Seasonal cycles of O_2, NO_3^- and SO_4^{2-} reduction in estuarine sediments: The significance of an NO_3^- reduction maximum in spring. Mar. Ecol. Prog. Ser. **24:** 65–74.

KRISTENSEN, E., M. H. JENSEN, AND R. C. ALLER. 1991. Direct measurement of dissolved inorganic nitrogen exchange and denitrification in individual Polychaete *Nereis virens* burrows. J. Mar. Res. **49:** 355–378.

LEUCHS, H. 1986. The ventilation activity of *Chironomus* larvae (Diptera) from shallow and deep lakes and the resulting water circulation in correlation to temperature and oxygen conditions. Arch. Hydrobiol. **108:** 281–299.

LEWANDOWSKI, J., AND M. HUPFER. 2005. Effect of macrozoobenthos on two-dimensional small-scale heterogeneity of pore water phosphorus concentrations in lake sediments: A laboratory study. Limnol. Oceanogr. **50:** 1106–1118.

LI, Y. H., AND S. GREGORY. 1974. Diffusion of ions in sea water and in deep-sea sediments. Geochim. Cosmochim. Acta **38:** 703–714.

LIIKANEN, A., AND OTHERS. 2003. Spatial and seasonal variation in greenhouse gas and nutrient dynamics and their interactions in the sediments of a boreal eutrophic lake. Biogeochemistry **65:** 83–103.

MEILE, C., K. TUNCAY, AND P. VAN CAPPELLEN. 2003. Explicit representation of spatial heterogeneity in reactive transport models: Application to bioirrigated sediments. J. Geochem. Explor. **78–79:** 231–234.

MENGIS, M., R. GACHTER, AND B. WEHRLI. 1997. Sources and sinks of nitrous oxide (N_2O) in deep lakes. Biogeochemistry **38:** 281–301.

NEUMANN, D., M. KRAMER, I. RASCHKE, AND B. GRÄFE. 2001. Detrimental effects of nitrite on the development of benthic *Chironomus* larvae, in relation to their settlement in muddy sediments. Arch. Hydrobiol. **153:** 103–128.

NIELSEN, O. I., B. GRIBSHOLT, E. KRISTENSEN, AND N. P. REVSBECH. 2004. Microscale distribution of oxygen and nitrate in sediment inhabited by *Nereis diversicolor*: Spatial patterns and estimated reaction rates. Aquat. Microb. Ecol. **34:** 23–32.

PELEGRI, S. P., AND T. H. BLACKBURN. 1995. Effect of bioturbation by *Nereis* sp., *Mya arenaria* and *Cerastoderma* sp. on nitrification and denitrification in estuarine sediments. Ophelia **42:** 289–299.

PINA-OCHOA, E., AND M. ALVAREZ-COBELAS. 2006. Denitrification in aquatic environments: A cross-system analysis. Biogeochemistry **81:** 111–130.

POLERECKY, L., N. VOLKENBORN, AND P. STIEF. 2006. High temporal resolution oxygen imaging in bioirrigated sediments. Environ. Sci. Technol. **40:** 5763–5769.

REAL, M., M. RIERADEVALL, AND N. PRAT. 2000. *Chironomus* species (Diptera: Chironomidae) in the profundal benthos of Spanish reservoirs and lakes: Factors affecting distribution patterns. Freshw. Biol. **43:** 1–18.

REVSBECH, N. P. 1989. An oxygen microsensor with a guard cathode. Limnol. Oceanogr. **34:** 474–478.

RICCIARDI, A., F. G. WHORISKEY, AND J. B. RASMUSSEN. 1997. The role of the zebra mussel (*Dreissena polymorpha*) in structuring macroinvertebrate communities on hard substrata. Can. J. Fish. Aquat. Sci. **54:** 2596–2608.

RUSJAN, S., M. BRILLY, AND M. MIKOS. 2008. Flushing of nitrate from a forested watershed: An insight into hydrological nitrate mobilization mechanisms through seasonal high-frequency stream nitrate dynamics. J. Hydrol. **354:** 187–202.

RYSGAARD, S., R. N. GLUD, N. RISGAARD-PETERSEN, AND T. DALSGAARD. 2004. Denitrification and anammox activity in Arctic marine sediments. Limnol. Oceanogr. **49:** 1493–1502.

SOETAERT, K., P. M. J. HERMAN, AND J. J. MIDDELBURG. 1996. A model of early diagenetic processes from the shelf to abyssal depths. Geochim. Cosmochim. Acta **60:** 1019–1040.

SOMMER, U. 1989. Nutrient status and nutrient competition of phytoplankton in a shallow, hypertrophic lake. Limnol. Oceanogr. **34:** 1162–1173.

SOSTER, F. M., AND P. L. MCCALL. 1990. Benthos response to disturbance in Western Lake Erie—field experiments. Can. J. Fish. Aquat. Sci. **47:** 1970–1985.

STIEF, P., AND D. DE BEER. 2002. Bioturbation effects of *Chironomus riparius* on the benthic N-cycle as measured using microsensors and microbiological assays. Aquat. Microb. Ecol. **27:** 175–185.

———, AND ———. 2006. Probing the microenvironment of freshwater sediment macrofauna: Implications of deposit-feeding and bioirrigation for nitrogen cycling. Limnol. Oceanogr. **51:** 2538–2548.

———, AND G. ELLER. 2006. The gut microenvironment of sediment-dwelling *Chironomus plumosus* larvae as characterised with O_2, pH, and redox microsensors. J. Comp. Physiol. B **176:** 673–683.

———, M. POULSEN, L. P. NIELSEN, H. BRIX, AND A. SCHRAMM. 2009. Nitrous oxide emission by aquatic macrofauna. Proc. Natl. Acad. Sci. USA **106:** 4296–4300.

SVENSSON, J. M. 1998. Emission of N_2O, nitrification and denitrification in a eutrophic lake sediment bioturbated by *Chironomus plumosus*. Aquat. Microb. Ecol. **14:** 289–299.

———, AND L. LEONARDSON. 1996. Effects of bioturbation by tube-dwelling chironomid larvae on oxygen uptake and denitrification in eutrophic lake sediments. Freshw. Biol. **35:** 289–300.

Sweerts, J. P. R. A., and D. De Beer. 1989. Microelectrode measurements of nitrate gradients in the littoral and profundal sediments of a meso-eutrophic lake (Lake Vechten, The Netherlands). Appl. Environ. Microbiol. **55:** 754–757.

Wall, L. G., J. L. Tank, T. V. Royer, and M. J. Bernot. 2005. Spatial and temporal variability in sediment denitrification within an agriculturally influenced reservoir. Biogeochemistry **76:** 85–111.

Walshe, B. M. 1947. Feeding mechanisms of *Chironomus* larvae. Nature **160:** 474–476.

Wang, F., A. Tessier, and L. Hare. 2001. Oxygen measurements in the burrows of freshwater insects. Freshw. Biol. **46:** 317–327.

Wright, J. F., P. D. Hiley, and A. D. Berrie. 1981. A 9-year study of the life cycle of *Ephemera danica* Mull (Ephemeridae, Ephemeroptera) in the River Lambourn, England. Ecol. Entomol. **6:** 321–331.

Associate editor: Ronnie Nøhr Glud

Received: 01 June 2009
Accepted: 25 November 2009
Amended: 13 November 2009